Test of Continuous Prestressed Concrete Girders Without End Blocks

GIRISH HIREMATH, RAFIK ITANI, AND UMESH VASISHTH

This study investigates the feasibility of eliminating end blocks from pretensioned continuous bridge girders. The removal of end blocks is estimated to reduce girder cost by 5 to 10 percent. The girders studied are the Washington State Department of Transportation (WSDOT) Series 14 type, which are characterized by 5-in.-thick webs. Previous research has recommended the elimination of end blocks for simple span bridges. A controlled laboratory test on two 20-ft-long Series 14 girders is performed. The girders are without end blocks and continuous throughout the deck. Their joint details are similar to those normally used in the field. At the continuous end, strains induced in the stirrups are monitored during the detensioning process and during various stages of loading. The load is applied at a distance of 13 ft 10 in. from the continuous end. The limiting load at which the flexural steel yielded is 408 kips. The maximum applied load is 480 kips, which is 54 percent higher than the ultimate design shear of 325 kips. At ultimate design shear, the deflection of the free end is 1.2 in. Even though the nominal strength of the concrete in the diaphragm is less than that of the girder, the cracks have been restricted to the girders. The maximum 28-day compressive strength of the concrete in the diaphragm is 4,000 psi, as compared to the 9,880 psi of the girders. It is concluded that the modified girders perform effectively under applied loads and hence warrant the removal of end blocks.

The structural efficiency and cost effectiveness of prestressed concrete has made its use advantageous in long span bridges. For bridges with unusual layouts and long spans, the post-tensioning method of prestressing has been widely adopted. Otherwise, precast and pretensioned concrete girders have been used for spans between 40 and 140 ft.

For many years bridge girders have contained enlarged webs at their ends over the transitional lengths. These enlargements are known as end blocks. End blocks are thought to be necessary for the distribution of prestressing force. Their construction requires special formwork, which contributes as much as 5 to 10 percent to the total cost. Therefore, end blocks are both uneconomical and undesirable and, if possible, should be omitted from pretensioned girders.

End blocks have been used because of concern over the bursting stresses in the end regions. However, since the prestressing force is transferred through the bond between the concrete and the strands, end blocks may not be required for pretensioned girders. In fact, researchers have concluded that satisfactory performance can be obtained if adequate stirrup reinforcement is provided (1–3). The state of Washington has, however, retained end blocks as a measure of safety.

The reason for retaining them is that the Washington series of girders have a higher-depth-to-web thickness ratio than the comparable AASHTO girders or those used in previous research.

Precast, pretensioned girders are often used in combination with a cast-in-place (CIP) deck. The CIP deck is an efficient structural system because it produces continuity for resisting live loads. The elimination of end blocks would reduce the area of cross section available for shear transfer at the continuous support.

This article describes an experimental study in which a continuous CIP deck and Washington State Department of Transportation (WSDOT) Series 14 girders without end blocks were subjected to ultimate shear and bending moment. The performance of the end regions of the girders at the continuous joint was monitored for crack propagation and stresses.

EXPERIMENTAL SETUP

WSDOT Series 14 girders are used for spans of 120 to 140 ft. These girders are characterized by their 73.5-in. depth and 5-in. web thickness (Figure 1). They are usually designed for an ultimate shearing force of 325 kips (4). Table 1 shows the design loads at a continuous joint for a span of 132 ft 10 in.

With these loads as the basis, two 20-ft Series 14 girders without end blocks were designed and erected on a concrete pedestal to form a typical continuous joint. The experimental setup is shown in Figure 2. Details of the girders and the continuous joint are shown in Figures 3 and 4.

The stirrups within Girders A and B were instrumented with strain gauges. A #4 steel bar was placed at the center and 3 in. from the bottom so that the stresses could be monitored in the vicinity of the end regions. Figure 5 shows the locations and numbers of the gauges on the stirrups and the steel bars. Symmetric instrumentation was used for Girder B, with 200 designations for gauges; for example, gauges 101 and 201 were in identical locations of Girder A and Girder B, respectively.

The strains were measured during detensioning, immediately after the slab and the diaphragm were cast, and during the load application. Before each event strain gauges were initialized.

G. Hiremath and Rafik Itani, Department of Civil and Environmental Engineering, Washington State University, Pullman, Wash. 99164-2910. U. Vasishth, Washington State Department of Transportation, Olympia, Wash. 98504. Current address: 1858 Lakemoor Place, Olympia, Wash. 98502.

OBSERVATIONS AND RESULTS

This section discusses the stresses and the strains during the prestress transfer caused by the applied loads. It also presents
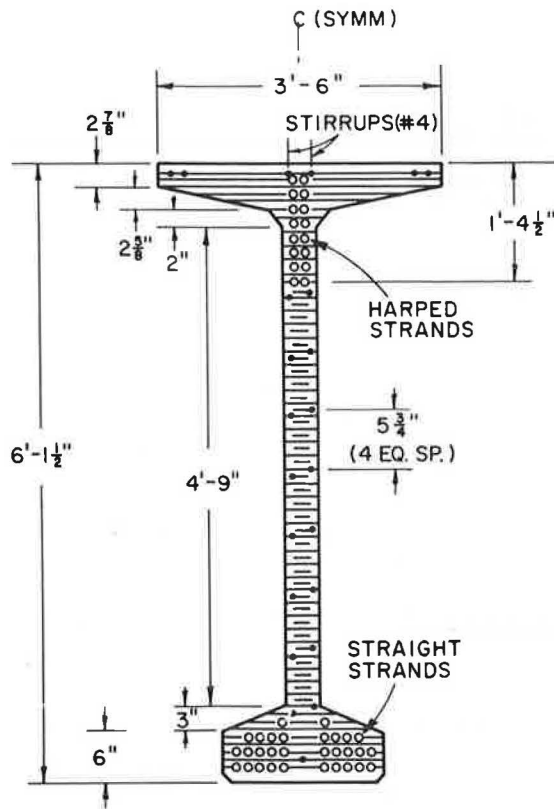
FIGURE 1   View of the continous end of a test girder.

the results of the combined effect of detensioning, casting of the slab and the diaphragm, and the applied loads.

During Prestress Transfer

The stresses in the stirrups and the longitudinal steel bar were obtained through the multiplication of the strains by the modulus of elasticity of steel ($E = 29,000$ ksi). Figures $6a–c$ show the variation in the stresses along the length of the girders. The following observations were made:

- The stress in the stirrups decreased with an increase in the distance from the ends of Girders A and B.
- Near the girder ends and at the levels of the centroidal axis, the stress was approximately 20 ksi (Figure $6a$). At the locations of the resultant prestressing force and juncture between the web and bottom flange, the stresses were 23 ksi (Figures $6b$ and $6c$). The stresses decreased with an increase in the distance, except at Gauges 230; 123 and 223; and 131 and 231, where the stresses varied from 20 ksi to 29 ksi.
- Stresses greater than 3.5 ksi indicated the presence of microcracks in the concrete. This was based on the assumption that the tensile strength of concrete is $7.5 \sqrt{f'c}$ and the modulus of elasticity of concrete is $33\ w^{1.5} \sqrt{f'c}$.
- The stresses in Girders A and B agreed well except at the junction of the web and the bottom flange. The region was highly susceptible to microcracking and the subsequent nonuniform behavior of concrete.

TABLE 1   DESIGN LOADS AT A CONTINUOUS SUPPORT

Case	Maximum Moment Case (ft-kips)	Maximum Shear Case (kips)
Vdl	99.	99.
VDL cont.	35.	35.
Vll	34.	45.
Vu	250.	274.
Mdl	-952.	-952.
Mll	-1067.	-804.
Mu	-3554.	-2980.

DL (Uniform Continuous) = 0.43 K/ft.
Impact = 1.194
Distribution = .955
Span = 132.8 ft.

Where, Vdl = factored dead load, kips

     Vdl cont. = factored uniform continums dead load, kips

          Vll = factored live load, kips

           Vu = design factored load, kips

         Mdl = factored moment due to dead load, ft-kips

         Mll = factored moment due to live load, ft-kips
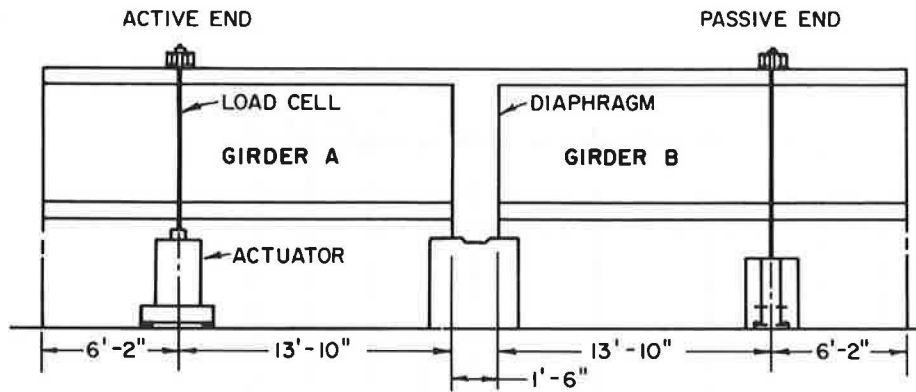
          Mu = design factored moment, ft-kips
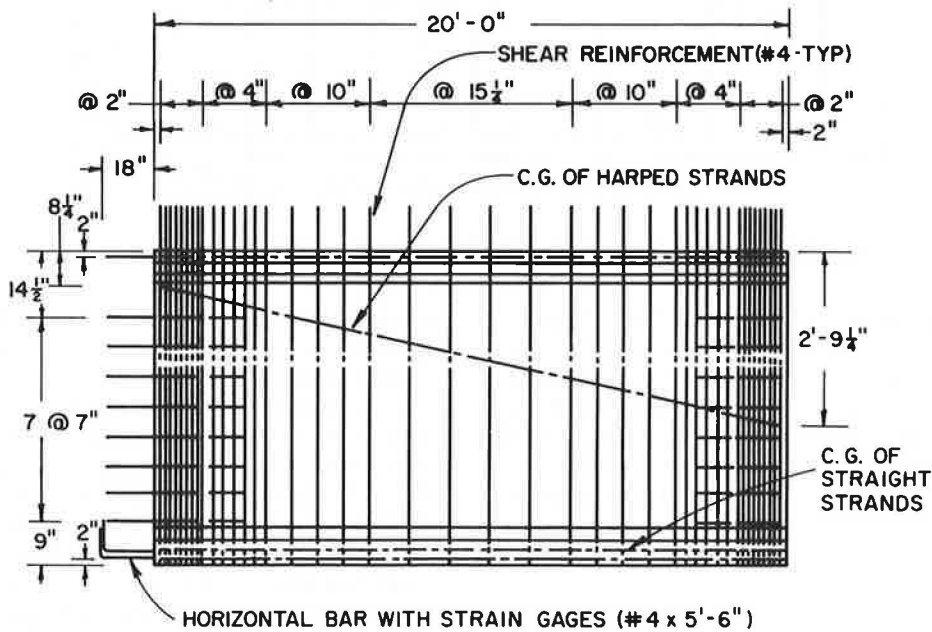
FIGURE 2   Elevation of the experimental setup.

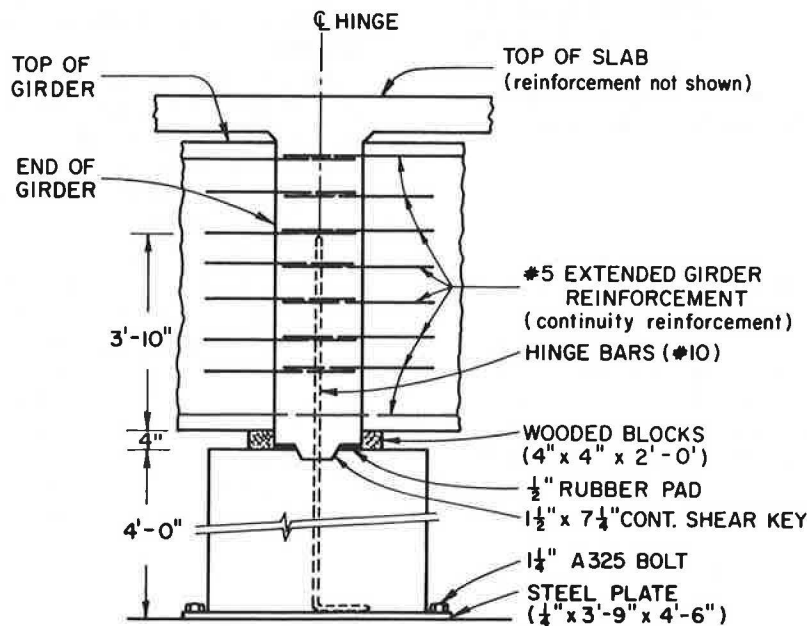**FIGURE 3**   Longitudinal section of a test girder.

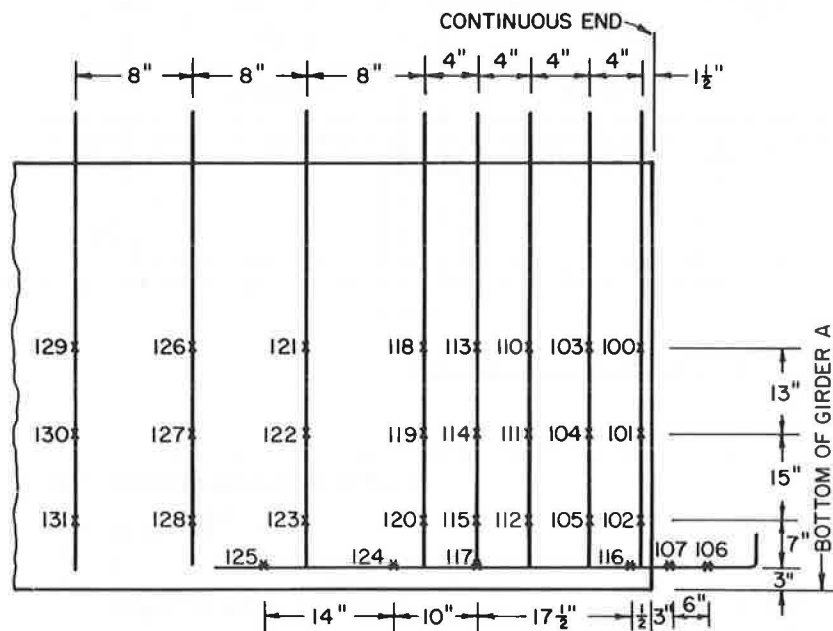**FIGURE 4**   Details of the continuous joint.

FIGURE 5 Configuration of strain gauges on stirrups of Girder A.

Figure 7 shows the stresses in the #4 steel bar at different locations along its length. The tensile stresses varied between 2 and 4 ksi and were considerably lower than those in the stirrups because the bar was outside the spalling and bursting zones. In addition, the bar was oriented in the direction of the cracks caused by spalling and bursting stresses. The compressive zone began at a distance of 28 in., which was beyond the transition zone of 25 in. from the end.

During Applied Loads

The results from the tests were independent of the strains recorded after detensioning and during the casting of the slab and diaphragm. The first applied load was 30 kips. This was followed by increments of 60 kips up to a load of 210 kips. At that level the increments were then decreased to 30 kips until a load of 510 kips was reached. At each load step the deflection at the point of loading and the strains were recorded.

Cracking Pattern

No significant cracking was observed until a load of 150 kips was reached. At that stage, cracks that had begun at detensioning propagated. The greatest increase in the length of the cracks was about 6 in. These were predominantly in the direction of the inclined prestressing strands in the webs. Vertical cracks caused by flexural stresses were noticed in the slab and the top flanges when a load of 210 kips was reached. Some of these cracks propagated into the webs as the load was increased to 270 kips. At that load lead, cracking was more prominent in the webs than in the slabs and the top flanges. These were on the tension side and within a distance of $h/4$ from the diaphragm, where h was the overall depth of the composite section. Up to this stage the flexural and the flex-

ure-shear cracks had been more dominant than those caused by web shear. The cracks were inclined at angles varying between 50 and 90 degrees.

As the load was increased, new cracks formed and earlier cracks extended. The cracks appeared to be equally spaced in the longitudinal direction and located away from the diaphragm. For loads higher than 300 kips, the cracks were mostly caused by web shear. At 300 kips, the cracks extended toward the bottom flange. Loads of 300, 330, and 360 kips created cracks that were located beyond a distance of $h/2$ from the ends and inclined at angles between 30 and 35 degrees. Similar cracking patterns were observed in both girders.

The observations made are summarized below:

- Cracks in the slab and top flange were caused by excessive flexural tensile stresses. The first visible flexural crack formed at an applied load of 210 kips.
- At an applied load of 270, the cracks were mainly caused by flexural shear. These were generally on the tension side of the web and fell within a distance of $h/4$ from the girder. The applied load of 270 kips corresponded to a maximum shear of 291 kips, which was higher than the design ultimate shear of 274 kips (Table 1).
- Cracks within a distance $h/2$ from the face of the diaphragm were inclined at varying angles, depending on their location with respect to the neutral axis. Cracks in the tension zone were inclined at an angle between 40 and 50 degrees to the horizontal. Cracks in the compression zone were inclined at an angle of 25 to 30 degrees. Thus, in the tensile region, flexural-shear cracks occurred, whereas in the compression region cracks were caused by shear stresses combined with direct and flexural-compressive stresses.
- For cracks farther away than $h/2$, the angle of inclination varied from 25 to 30 degrees. These cracks were caused by loads of more than 270 kips. Cracks caused by loads of 270, 360, 390, 420, 450, and 480 kips were located 1 ft 6 in., 3 ft, 3 ft 8 in., 6 ft 3 in., 10 ft, and 10 ft 3 in. from the face of the
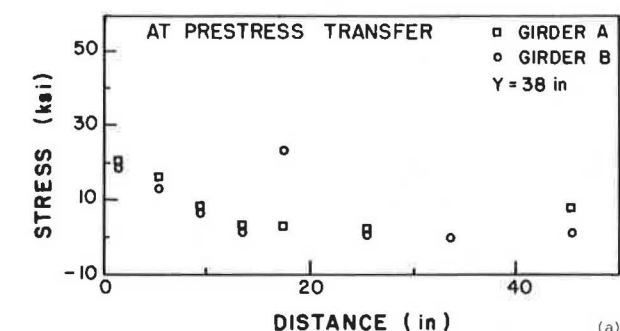
Y = DISTANCE FROM THE BOTTOM OF THE GIRDERS
TO THE CENTROIDAL AXIS
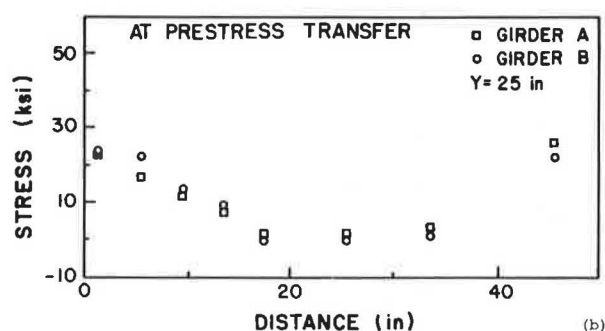
Y = DISTANCE FROM THE BOTTOM OF THE GIRDERS
TO THE RESULTANT PRESTRESSING FORCE
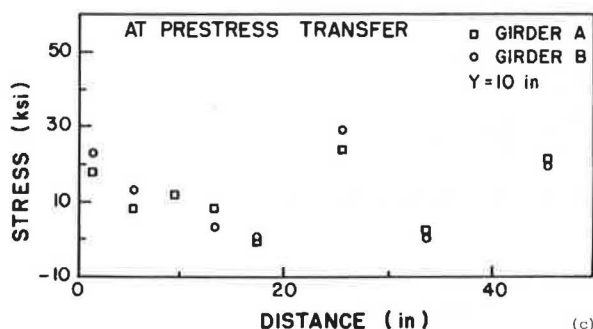
Y = DISTANCE FROM THE BOTTOM OF THE GIRDERS
TO THE JUNCTION OF THE BOTTOM FLANGE AND
THE WEB

FIGURE 6 **Stresses in stirrups versus distance from the continuous end at the (a) centroidal axis, (b) resultant prestressing force, and (c) junction of the flange and the web.**

diaphragm and along the centroidal axis. The corresponding angles of inclination at these locations were 65, 50, 35, 30, 29, and 25 degrees.

• Most of the web-shear cracks originated at the junction of the top flange and web and propagated toward the bottom flange at an angle of 30 degrees. Web-shear cracking was observed at loads higher than 300 kips.

Strains recorded during the test were caused by only the applied loads because the gauges had been initialized before loading. A sudden increase in strain in a gauge is a result of
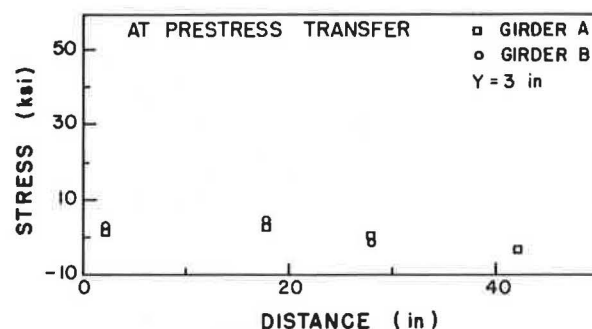
Y = DISTANCE FROM THE BOTTOM OF THE GIRDERS TO THE
HORIZONTAL BAR AT THE CENTER OF THE BOTTOM
FLANGE

FIGURE 7 **Stresses in the horizontal bar at the center of the bottom flange versus distance from the continuous end.**

cracking in the concrete and the subsequent transfer of loads to the stirrup.

Strains Versus Applied Loads

The variation in strains in the gauges that occurred as the applied load increased from 30 to 480 kips is discussed in the following subsections.

Gauges on the Stirrups

In Figures 8 and 9, strains versus applied loads are plotted for the gauges on the stirrups located 38 in. from the bottom of the girders.

Figure 8 shows (Gauges 100 and 200) the presence of microcracks at a load of 150 kips. For loads greater than 150 kips, the strain increased. Gauge 213 indicated the formation of microcracks at a load of 270 kips, whereas for loads greater than 270 kips, Gauge 113 showed a rapid increase in strains. The gauges shown in Figure 8 were located below the centroidal axis of the composite section.

Figure 9 shows that Gauges 118 and 218 behave linearly up to a load of 300 kips, whereas Gauges 129 and 229 show a linear response up to 360 kips. At loads of more than 300 and 360 kips, respectively, concrete cracking transferred the load to the stirrups.

The response of the stirrups at the level of the resultant prestressing force, that is, 25 in. from the bottom of the girders, can be seen in Figures 10 and 11.

Figure 10 shows that deviation occurs at a load of 270 kips. In the case of Gauges 114 and 214, there was a transition from a compressive strain to a tensile strain. For Gauges 122 and 222, deviation from linearity occurred at a load of 360 kips.

For Gauges 127 and 227 (Figure 11) the cracking load was 360 kips. Gauge 130 indicated a linear increase in tensile strains of up to a load of 390 kips and then deviated from linearity. Gauge 230 did not function.

The strains in the gauges at the junction of the web and the bottom flange are plotted in Figures 12 and 13.

Gauges 105 and 205, shown in Figure 12, indicated com-

FIGURE 8   Stresses in the stirrups due to applied loads—Gauges 100, 200, 113, and 213.

FIGURE 9   Stresses in the stirrups due to applied loads—Gauges 118, 218, 129, and 229.

FIGURE 10   Stresses in the stirrups due to applied loads—Gauges 114, 214, 122, and 222.

FIGURE 11   Stresses in the stirrups due to applied loads—Gauges 127, 227, 130, and 230.
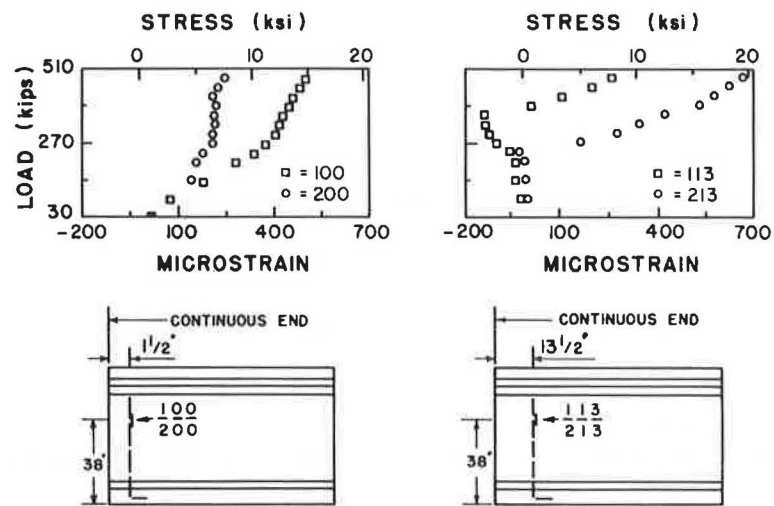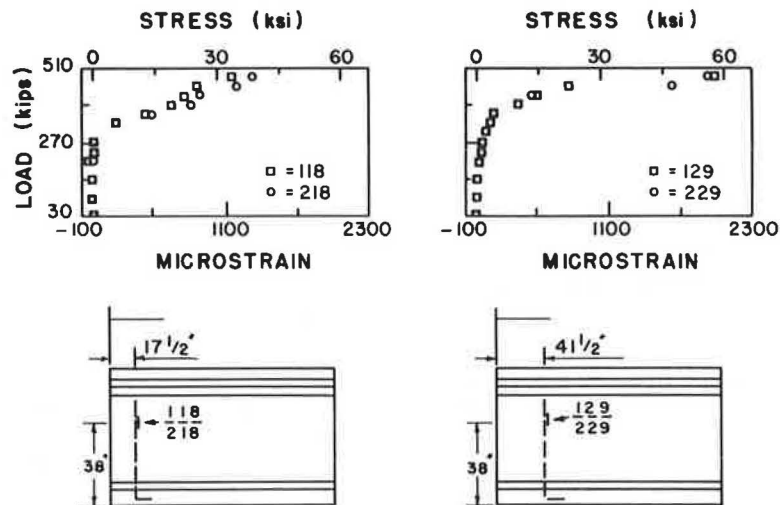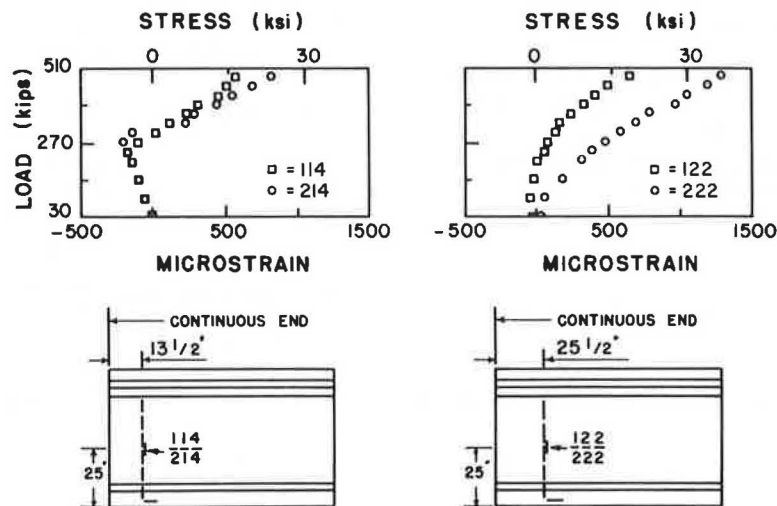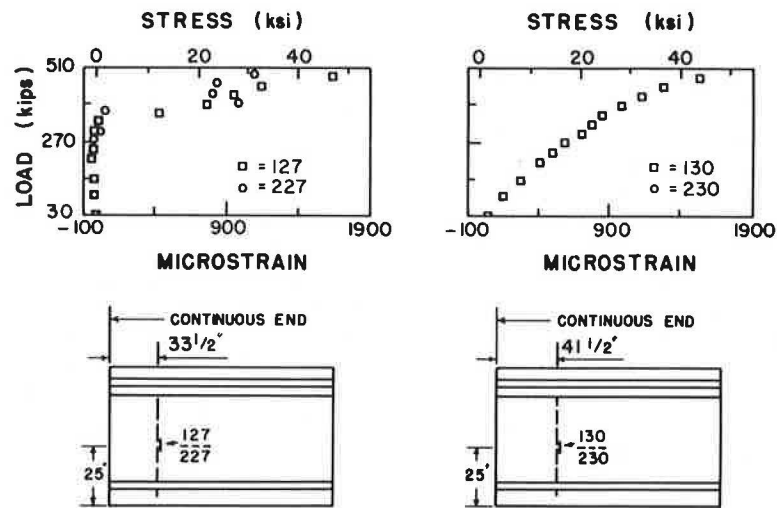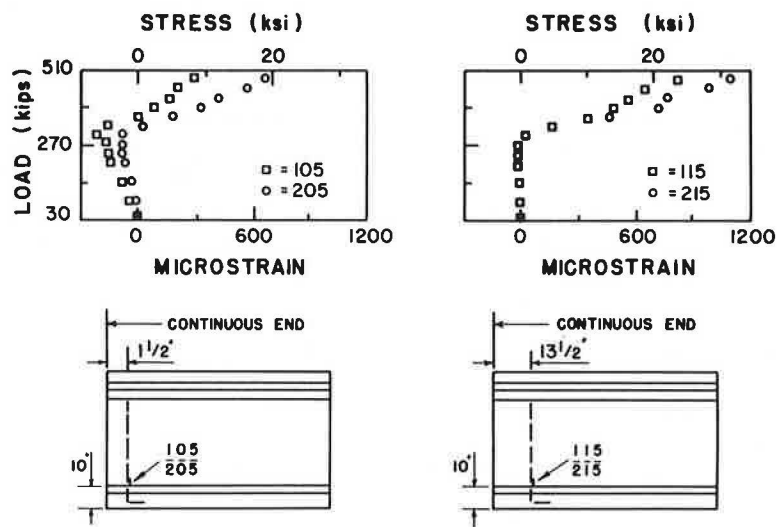
FIGURE 12   Stresses in the stirrups due to applied loads—Gauges 105, 205, 115, and 215.
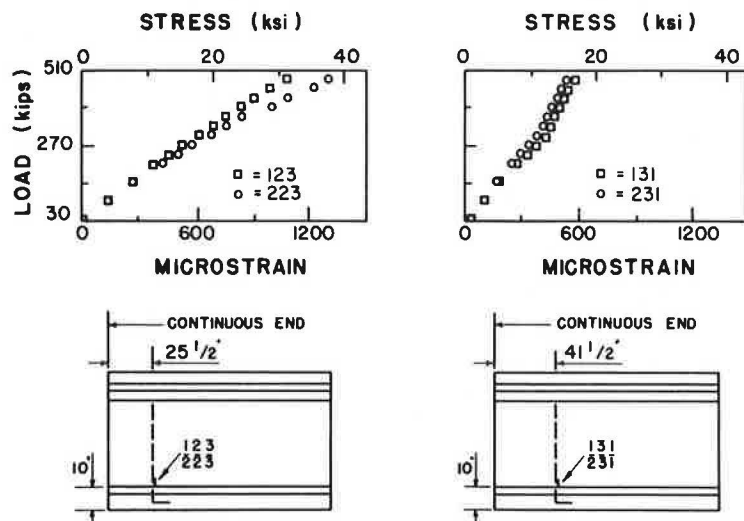
FIGURE 13   Stresses in the stirrups due to applied loads—Gauges 123, 223, 131, and 231.

pressive strain, whereas Gauges 115 and 215 showed negligible strains up to a load of 300 kips. Beyond that point, the strains became increasingly tensile. Figure 13 shows that Gauge 123 behaved linearly up to a load of 480 kips, whereas Gauge 223 deviated from linearity at 360 kips. The steady increase of tensile strains in the gauges was caused by the strutting behavior of the concrete. Strutting action caused the stirrups to be in tension. The results agreed with the cracks observed near the web and the bottom flange.

The following conclusions can be drawn from the strains in the stirrups:

● Loads at which the strain-versus-load curve deviate from linearity increased for gauges located farther away from the diaphragm.
● Generally gauges located within 13.5 in. from the diaphragm showed good agreement at loads less than 270 kips.
● In general, gauges located beyond 13.5 in. behaved linearly up to a load of 300 kips.

Strains Along the Center of the Bottom Flange

Strains in the steel bar located 3 in. above and along the centerline of the bottom flange are presented in Figures 14 to 16.

Gauges 106, 206, 107, and 207 were located within the diaphragm. Therefore, they indicated compressive strains (Figure 14). Figures 15a and 15b compare experimental and theoretical values as obtained by the flexural equation.

The theoretical values were based on the assumptions that concrete acts as a homogeneous and linearly elastic material. Tensile reinforcement in the slab was transformed into an equivalent area of concrete. The deviation of the experimental values from the theoretical results began at a load of 270 kips.

Figure 16 shows the development of cracks at Gauges 124 and 224 and at a load of 330 kips. Gauge 225 did not function,

whereas Gauge 125 deviated from linearity at a load of 270 kips.

The strains in the steel bar lead to the following conclusions:

● The maximum compressive strain at the midsection of the diaphragm was 0.0017, which was about 50 percent of the maximum compressive strain that concrete can sustain.
● The tension in Gauges 124, 224, and 125 can be explained on the basis of the compression strut theory. The formation of cracks in the web near the bottom flange resulted in a strutting action in the web. The horizontal component of the force in the strut was resisted by the bottom flange, which behaved as a tension member.

Combined Effective Strains and Stresses

In the previous subsection, the strains and stresses caused by applied loads and corresponding moments were studied. This subsection presents the combined strains resulting from the effective prestressing force and the slab. Tables 2, 3, and 4, which assume a prestressing loss of 25 percent and a linear relationship between the prestressing force and stresses, show the combined effect of prestressing force, the weight of the slab, and the applied load.

Table 2 shows the stresses from gauges that are 38 in. from the bottom of the girders. At a load of 300 kips, the greatest stress in the stirrups was 20 ksi, and it occurred 1.5 in. from the diaphragm. Up to the applied load of 360 kips, stresses in the stirrups decreased as the distance from the diaphragm increased. For loads higher than 360 kips, stresses in the stirrups farther than 17.5 in. increased. At a load of 480 kips, the first yielding occurred in the stirrup located 41.5 in. from the diaphragm.

Table 3 shows the stresses that are located 25 in. from the bottom. Within a distance of 9.5 in., stresses increased as the distance from the diaphragm increased. The greatest stress at
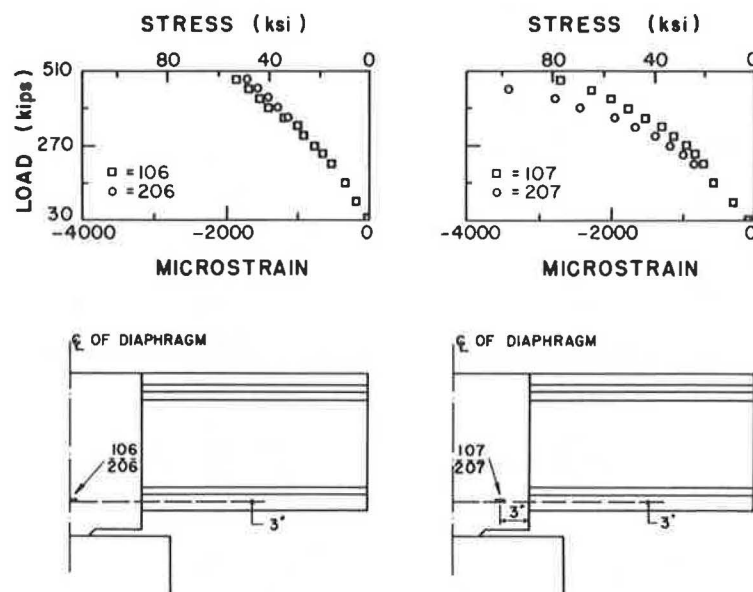

FIGURE 14 Stresses in the horizontal bar at the center of the bottom flange due to applied loads—Gauges 106, 206, 107, and 207.
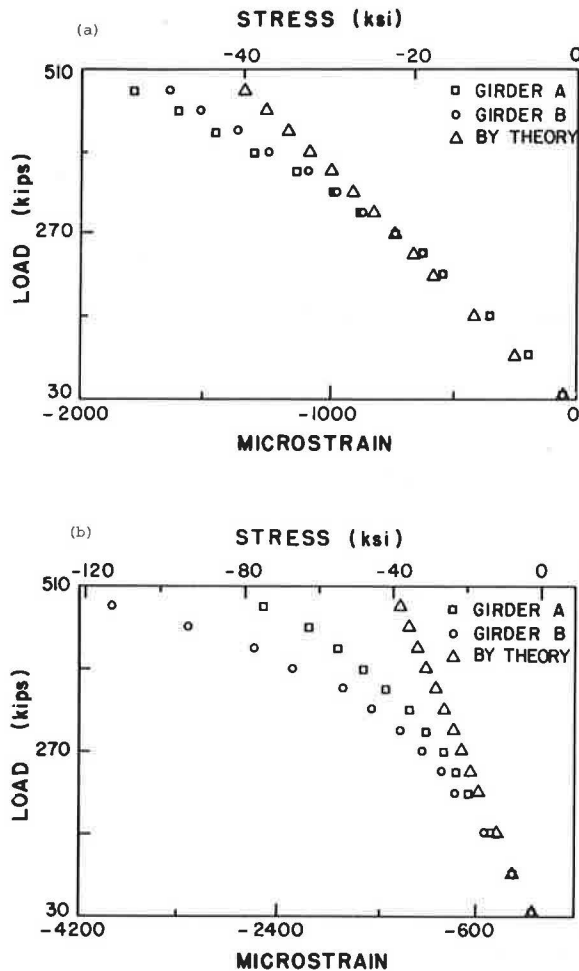
FIGURE 15 Comparison of the experimental and theoretical results—(a) Gauges 106 and 206 and (b) Gauges 107 and 207.

a load of 300 kips was 17 ksi and occurred at a distance of 25.5 in. Beyond that load and except for gauges 222 and 127, the stresses decreased. At the maximum load of 480 kips, stresses in the stirrups located within the transfer length of 25 in. were about 50 percent of the yield stress. At that load level, yielding occurred in the stirrup located 25.5 in. from the diaphragm.

At the junction of the web and the bottom flange, that is, 11 in. from the bottom, and at a load of 300 kips, the maximum stress in the stirrups was 17 ksi and occurred at 33.5 in. (Table 4). At 480 kips, the stresses within a distance of 17.5 in. were within 50 percent of the yield stress, whereas stresses at 33.5 in. were 57 ksi.

Table 5 shows the maximum stresses in the stirrups along the length of the girders. The following data can be observed from the table.

- The maximum stress at a load of 300 kips was 20 ksi and occurred at 1.5 in. from the end of the girder. That stress is 33 percent of the yield stress (60 ksi).
- Within the transfer length of 25 in., the maximum stress caused by a load of 480 kips was 36 ksi, which was about 60 percent of the yield strength. For locations beyond the transfer length, the maximum stress at 480 kips was 60 ksi.
- As the load increased from 300 kips to 480 kips, the stresses increased with an increase in the distance from the diaphragm.

Load Versus Deflection Curve

The deflection of the active side was measured at the point of load application. Figure 17 shows a curve of load versus deflection. The curve is linear up to 270 kips of applied load. Thereafter, deflection increased steadily with an increase in the applied load. The maximum deflection was 3.3 in., whereas the deflection at 270 kips was 1.2 in. The recovery after the
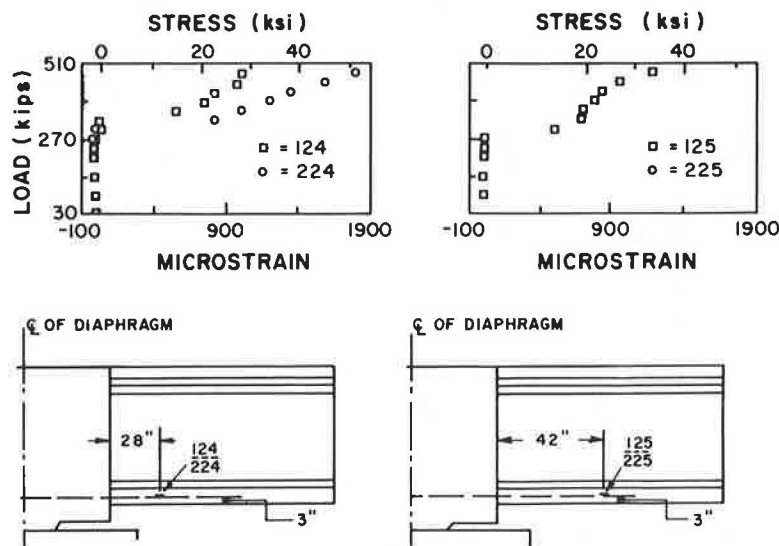

FIGURE 16 Stresses in the horizontal bar at the center of the bottom flange due to applied loads—Gauges 124, 224, 125, and 225.

TABLE 2   STRESSES (ksi) IN STIRRUPS AT $y = 38$ in. LOAD COMBINATION: EFFECTIVE PRESTRESS PLUS WEIGHT OF THE SLAB PLUS THE APPLIED LOAD

	x															
	1.5		5.5		9.5		13.5		17.5		25.5		33.5		41.5	
	Girder															
	A	B	A	B	A	B	A	B	A	B	A	B	A	B	A	B
	Gage No.															
Load (kips)	100	200	103	203	110	210	113	213	118	218	121	221	125	226	129	229
30	10	10	9	7		5		1	2		1	-1			6	
90	14	13	1	3		2		1	2		1	-1			6	
150	14	13	1	3		2		1	2		2	0			7	
210	17	14	0	-1		2		1	2		3	0			7	
240	18	14	-2	-2		3		1	3		3	1			8	
270	19	15	-3	-4	NG	2	NG	6	3	NG	4	1	NG	NG	8	NG
300	20	15	-3	-4		3		9	7		8	3			9	
330	20	15	-3	-5		4		11	8		12	8			11	
360	21	15	-2	-4		7		13	15		19	9			11	
390	21	15	-2	-2		10		16	21		27	18			16	
420	21	15	-1	-3		11		17	23		29	29			20	
450	22	15	-1	-5		13		18	26		33	37			27	
480	23	16	-2	-5		15		19	34		44	43			60	

x = distance of a stirrup from the face of the diaphragm in inches

y = distance of the gases from the bottom of girder A and girder B

NG = Not Good

TABLE 3   STRESSES (ksi) IN STIRRUPS AT $y = 25$ in. LOAD COMBINATION: EFFECTIVE PRESTRESS PLUS WEIGHT OF THE SLAB PLUS THE APPLIED LOAD

	x															
	1.5		5.5		9.5		13.5		17.5		25.5		33.5		41.5	
	Girder															
	A	B	A	B	A	B	A	B	A	B	A	B	A	B	A	B
	Gage No.															
Load (kips)	101	201	104	204	111	211	114	213	119	219	122	222	127	227	130	230
30	7		11	11	10	8	6	6	-1	-1	-6	1	-2			
90	5		9	10	8	7	4	5	-1	-2	-6	3	-2			
150	2		7	7	6	6	4	4	-1	-3	-5	6	-3			
210	1		5	6	4	5	2	2	-2	-5	-5	10	-3			
240	1		4	5	2	4	1	2	-2	-5	-3	12	-3			
270	2	NG	4	4	3	10	3	0	-2	-8	-3	14	-3			
300	2		5	4	7	14	7	2	0	1	-1	17	-2			
330	3		6	5	9	16	9	12	8	5	-1	20	-1			
360	5		6	5	9	17	13	13	13	5	1	23	10			
390	7		7	9	10	20	15	18	15	8	4	27	19			
420	8		8	11	10	21	19	21	17	13	6	30	24			
450	9		8	13	11	23	20	25	18	17	8	33	29			
480	10		9	15	13	25	22	28	20	19	12	60	42			

x = distance of a stirrup from the face of the diaphragm in inches

y = distance of the gases from the bottom of girder A and girder B
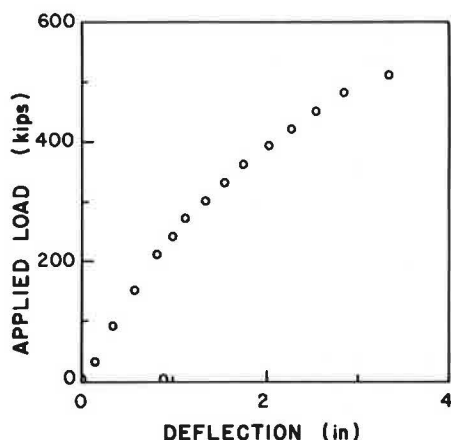
NG = Not Good

FIGURE 17 Applied loads versus deflection.

the first yielding of the stirrups occurred at an applied load of 480 kips, which corresponded to a total shear of 500 kips. The girders showed an excess capacity of 54 percent beyond the ultimate shear.

The first yielding of the longitudinal steel occurred at a moment of 5,407 ft-kips. The maximum ultimate design moment was 3,554 ft-kips, so the composite section had 52 percent excess moment capacity over the maximum design moment.

Therefore, the logical conclusion is that Series 14 girders without end blocks can perform effectively as continuous girders as long as (a) they are placed normal to the support and (b) the construction sequence presented in this paper is followed. Even though no impact or fatigue loadings were used, the conclusions should hold considering the high levels of factor of safety for ultimate moment and shear force.

REFERENCES

1. W. T. Marshall, and A. H. Mattock. Control of Horizontal Cracking in the Ends of Pretensioned Concrete Girders. *PCI Journal*, Vol. 7, No. 5, Oct. 1962, pp. 56–74.
2. P. Gergely, M. A. Sozen and C. P. Siess. *The Effect of Reinforcement on Anchorage Zone Cracks in Prestressed Concrete Members.* Structural Research Series 271. University of Illinois, Urbana, 1963.
3. N. M. Hawkins. Behavior and Design of End Blocks for Prestressed Concrete Beams. *Civil Engineering Transactions*, Institute of Engineers, Barton, Australia, Vol. CE8, No. 2, Oct. 1966.
4. *Bridge Design Manual Volume 1—Criteria.* Washington State Department of Transportation, Olympia, July 1982.
5. Precast-Prestressed Concrete Bridges (6 parts). *PCA Journal*, May 1960, Sept. 1960, Jan. 1961, May 1961, Sept. 1961.

TABLE 4   STRESSES (ksi) IN STIRRUPS AT $y = 11$ in. LOAD
COMBINATION: EFFECTIVE PRESTRESS PLUS WEIGHT OF THE
SLAB PLUS THE APPLIED LOAD

								x								
	1.5		5.5		9.5		13.5		17.5		25.5		33.5		41.5	
								Girder								
	A	B	A	B	A	B	A	B	A	B	A	B	A	B	A	B
								Gage No.								
Load (kips)	102	202	105	205	112	212	115	215	120	220	123	223	128	228	131	231
30	11	14	5	9	8		6	1	0	-13			2	-1		
90	10	14	5	9	8		6	1	0	-13			2	-1		
150	8	13	3	8	7		5	1	-1	-14			2	-1		
210	5	11	2	7	7		5	1	-1	-14			2	-1		
240	4	10	2	7	6		5	1	-1	-14			1	-1		
270	3	9	1	7	6	NG	5	1	-1	-14	NG	NG	1	-1	NG	NG
300	3	9	0	7	5		6	2	-1	-15			17	-1		
330	4	9	2	10	8		10	6	-1	2			40	18		
360	5	11	6	14	12		15	14	1	3			38	38		
390	6	12	8	18	13		19	21	18	11			41	41		
420	7	13	10	21	15		21	22	20	14			44	45		
450	6	14	11	25	16		24	28	24	22			49	52		
480	6	15	14	27	20	28	31	30	27	57			57	57		

x = distance of a stirrup from the face of the diaphragm in inches

y = distance of the gages from the bottom of girder A and girder B

NG = Not Good

TABLE 5   MAXIMUM STRESSES (ksi) IN THE STIRRUPS

X	1.5	5.5	9.5	13.5	17.5	25.5	33.5	41.5
Load (kips)								
30	14	11	10	6	2	1	2	6
90	14	10	8	6	2	3	2	6
150	14	8	7	5	2	6	2	7
210	17	7	7	5	2	10	2	7
240	18	7	7	5	2	10	2	7
270	19	7	10	6	3	14	1	8
300	20	7	14	9	7	17	17	9
330	20	10	16	11	8	20	40	11
360	21	14	17	15	15	23	38	11
390	21	18	20	19	21	27	41	16
420	21	21	21	21	23	30	44	20
450	22	25	23	24	26	33	49	27
480	23	27	25	28	31	36	52	60

x = Distance from the face of the diaphragm

removal of the load was 2.4 in., that is, the net plastic deformation was 0.9 in.

SUMMARY AND CONCLUSIONS

The Series 14 girders have been statically tested and designed for a maximum factored shear, V_u, of 274 kips and a moment, M_u, of 3,552 ft-kips. The maximum ultimate shear, V_u, for Series 14 girders is equal to 325 kips. This is approximately equal to an applied test load of 300 kips, in addition to the maximum manufactured dead load shear of 21 kips. At that shear force, the maximum effective stress in the stirrups was 20 ksi, which was 33 percent of yield stress. That load corresponded to the initiation of web cracking.

At higher loads, web cracking increased, and the stirrups located beyond the transfer length of 25 in. indicated higher stresses than those located within the transfer length. Finally,